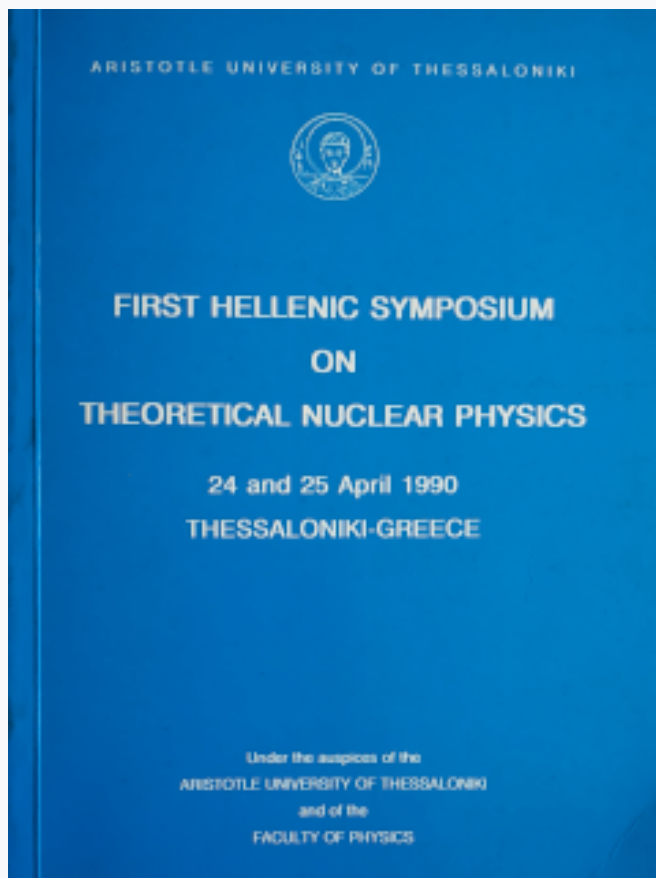


HNPS Advances in Nuclear Physics

Vol 1 (1990)

HNPS1990



Conditions for the existence of peaks in the Sigma hypernucleus spectra

Th. Petridou, C. Daskaloyannis

doi: [10.12681/hnps.2833](https://doi.org/10.12681/hnps.2833)

To cite this article:

Petridou, T., & Daskaloyannis, C. (2020). Conditions for the existence of peaks in the Sigma hypernucleus spectra. *HNPS Advances in Nuclear Physics*, 1, 144–155. <https://doi.org/10.12681/hnps.2833>

Conditions for the existence of peaks in the Sigma hypernucleus spectra *

Th.Petridou and C.Daskaloyannis

Department of Theoretical Physics

University of Thessaloniki

GR-54006, Thessaloniki, GREECE

Abstract: The (K^-, π^\pm) sigma hypernuclear spectrum is studied qualitatively in the Green function approach, using a solvable interaction model. The general features of the spectrum are explained. The necessary conditions for the existence of peaks in the spectrum are also studied. We show that the resonant peaks can be distinguished in the case of a real strong spin-orbit potential with a relatively weak Sigma to Lambda conversion.

1.Introduction

The Sigma production spectrum in the (K^-, π^\pm) interaction was experimentally studied by using in flight [1-5] or at rest [6-11] kaons. The early estimates of the data gave a small width, 5 to 10 MeV, to the Sigma-nucleus resonances [1,3,7]. This width was not confirmed in the subsequent experimental data [10], although the resonance structure reappears in the case of small Σ -hypernuclei as in ${}^4_\Sigma He$ [11].

Gal and his collaborators [12,13] proposed an explanation of the resonances with narrow width, using the UBS (Unstable Bound State) theory. Morimatsu and Yazaki [14], using the Green function method, have found a discrepancy between the position of the resonance peaks and the location of the UBS poles, specially when the imaginary part of the optical nucleus-hadron potential is strong enough. Gal [15] observed, that this disagreement depends on the position of the poles in the complex k-plane. Thus, it was concluded that the UBS theory cannot be used for the study of the resonant peaks in the pion spectrum, derived by the (K^-, π^\pm) production of the Sigma Hypernucleus. The general features of the pion spectrum are usually attributed to the quasi-free background [16,17].

The aim of this contribution is the qualitative study of the (K^-, π^\pm) spectrum. For this reason we use a square well potential with a delta spin-orbit interaction. The production strength (the response function) of the $(K, \pi^\pm)_\Sigma$ hypernucleus production can be written as the superposition of terms, each of them corresponding to a definite nucleon hole - hyperon configuration. Each term has the typical appearance of resonance, but in the case

* Presented by Th. Petridou

of the Sigma-hypernuclei these resonances are densely distributed above the threshold. When the resonances are prominent, we observe peaks in the spectrum.

The location of the poles of the hypernuclear Green function and the position of the observed peaks in the spectrum are related, but they do not coincide always. We observe that this coincidence depends on the relative size of the real part of the potential depth over the size of the imaginary part. The addition of a real strong spin orbit potential intensifies the real part of the total potential over the imaginary part, and the coincidence between the Green function poles and the resonant peaks becomes more prominent. We estimate the difference between the position of the resonant peaks and the poles.

The Green function method is analyzed in ref.[14] and [18]. This method takes into account the resonant and the continuum processes. Thus it is appropriate to describe the sigma hypernucleus production.

2. The model

The production strength $S(E)$ is given by the formula [14,18]:

$$S(E) = -\frac{1}{\pi} \text{Im}F(E) \quad (1)$$

In the case of the at-rest Kaon capture, the partial production rate is given by:

$$\Gamma(K^-(n_K \ell_K), Z^A \rightarrow \pi(k_\pi), \text{all}) = \frac{1}{2\ell_K + 1} \lambda \left[\frac{d\sigma}{d\Omega} \right]_{KN \rightarrow \Sigma\pi} \sum_{m_K} \int d\Omega_\pi S(E_K - E_\pi - E_r)$$

The averaged strength function $F(E)$ over the nuclear spin orientations is given by the formula:

$$F(E) = \sum_{\ell, j} F_{\ell, j}(E)$$

where:

$$F_{\ell, j}(E) = (2j + 1)(2j_N + 1) \sum_{\{L\}} (2L + 1) \begin{pmatrix} j_N & j & L \\ -1/2 & 1/2 & 0 \end{pmatrix}^2 f_{\ell, j}^L(E)$$

where $\{L\}$ denotes the summation over the permitted values of L such that $\ell_N + \ell + L = \text{even}$.

$$f_{\ell, j}^L(E) = \sum_M \int_0^\infty dr \int_0^\infty dr' [f_L^M(r)]^* G_{\ell, j}(E; r, r') f_L^M(r') \quad (2)$$

and the weight function $f_L^M(r)$ is:

$$f_L^M(r) = u_{\ell_N, j_N}(r) \int d\Omega Y_L^M(\hat{r}) [\chi_\pi(\bar{r})]^* \chi_K(\bar{r})$$

The $G_{\ell,j}(E; r, r')$ is the radial part of the Green function of the hyperon in the optical hyperon-nucleus potential corresponding to the $[\ell, j]$ sigma configuration. The $u_{\ell_N, j_N}(r)$ is the radial part of the nucleon wave function corresponding to the $[\ell_N, j_N]^{-1}$ hole configuration. The χ_π (or χ_K) is the pion (or the kaon) wave function in the pion-nucleus (or the kaon-nucleus) optical potential.

The Green function in eq.(2) corresponds to the Schrödinger equation

$$\frac{d^2 u}{dr^2} + \left\{ \left(\frac{2m}{\hbar^2} \right) [E - V(r)] - \frac{\ell(\ell + 1)}{r^2} \right\} u = 0 \quad (3)$$

where $V(r)$ is the optical potential, containing a central part and a spin orbit part. For the sake of simplicity, we consider the case of the Σ^0 hypernucleus, so that no Coulomb interaction appears.

$$V(r) = V_c w(r) + V_{so}(\vec{l} \cdot \vec{s}) r_o^2 \frac{1}{r} \frac{dw(r)}{dr}$$

The potential depths V_c and V_{so} are assumed to be complex. The imaginary part of the potential simulates the Sigma to Lambda conversion. The function $w(r)$ is the nucleon density normalized to unity at the origin. In the solvable model, adopted in this paper, the nucleon distribution is represented by a density of rectangular shape:

$$w(r) = \begin{cases} 1 & \text{if } r < R; \\ 0 & \text{if } r \geq R; \end{cases} \quad R = r_o A^{1/3} \quad (4)$$

and

$$\frac{dw(r)}{dr} = -\delta(r - R)$$

The Green function $G_{\ell,j}(E; r, r')$, corresponding to the Schrödinger equation (3), satisfies the equation:

$$G = G_c + G_c U_{so} G$$

where $U_{so} = -V_{so}(\vec{l} \cdot \vec{s}) r_o^2 (1/R) \delta(r - R)$ is the spin-orbit potential and G_c is the Green function of the central potential. For simplicity, we omit all the indices relative to angular momentum ℓ . This equation can be solved exactly and after a little algebra we find:

$$G_{\ell,j}(E, r, r') = G_c(E; r, r') - \frac{V_{so}(\vec{l} \cdot \vec{s}) r_o^2 (1/R) G_c(E; r, R) G_c(E; R, r')}{1 + V_{so}(\vec{l} \cdot \vec{s}) r_o^2 (1/R) G_c(E; R, R)} \quad (5)$$

In this paper, we consider the case of the at rest (K, π^-)-production of the C_{Σ}^{12} . The parameter r_o in eqn.(4) is taken to be 1.31 fm. The Kaon is assumed to be in the atomic 3d state. The pion interacts with the hypernucleus with the complex optical potential $\pi 1$ of the ref.[19] and for the nucleon-nucleus interaction the Bohr-Mottelson optical potential is used [18].

The strength function $f_{\ell,j}^L(E)$ given by eq.(2) can be written as follows:

$$f_{\ell,j}^L(E) = G_{\ell,j}(E; R, R) \Sigma_{\ell,j}^L(E) \quad (6)$$

where

$$\Sigma_{\ell,j}^L(E) = \sum_M \int_0^\infty dr \int_0^\infty dr' [f_L^M(r)]^* \left[\frac{\phi(r_<)}{\phi(R)} \frac{\psi^{(+)}(r_<)}{\psi^{(+)}(R)} \right] f_L^M(r') \quad (7)$$

The functions $\phi(r)$ and $\psi^{(+)}(r)$ are the regular and Jost solutions of the Schrödinger equation (3). The factor $G_{\ell,j}(E; R, R)$ is the origin of the resonant and continuum background of the spectrum and depends only on the hyperon-nucleus potential. The factor $\Sigma_{\ell,j}^L(E)$ depends essentially on the production mechanism ((K, π^\pm) or (π^\pm, K) , in-flight or at-rest) of the hypernucleus. This term is slowly dependent from the spin-orbit potential and does not contain any resonant behaviour, as we can see in fig.1. The function inside the brackets is equal to unity near the radius R , while the terms $f_L^M(r)$ tend to zero when $r \rightarrow \infty$.

The factor $\Sigma_{\ell,j}^L(E)$ is responsible for the general features of the quasi-free background of the spectrum as in ref. [16] and [17]. The Green function in eq.(6) generates the resonant peaks in the pion spectrum. Therefore, there must be some correlation between the poles of the Green function and the resonant peaks. In some cases there is a coincidence of the peaks and the poles, while in other cases this coincidence is not obvious, see ref. [14].

In fig.2, we can see that the entire pion spectrum can be regarded as a dense accumulation of resonances above the sigma threshold. These resonances depend on the nucleon-hole and sigma particle configurations. The appearance of the resonant peaks depends on the sharpness of the corresponding resonance in the particle-hole configuration. By the little arrows in fig.2, we indicate the position of the real part of the poles (E_{pole}). We remark that the location of the poles is clearly correlated to the energy positions (E_{peak}) of the $[p_{3/2}]_\Sigma$, $[d_{5/2}]_\Sigma$, $[f_{7/2}]_\Sigma$, ...peaks.

We can explain the discrepancy between the position of the peak (E_{peak}) and the location of the Green function pole (E_{pole}). For simplicity we consider a simple square well potential as in ref.[14]. The Green function is given by the formula:

$$G_{\ell,j}(E; R, R) = \frac{2m}{\hbar^2} \frac{1}{H(E)}$$

where

$$H(E) = pj'_\ell(pR)/j_\ell(pR) - kh'_\ell(kR)/h_\ell(kR)$$

where $p = \sqrt{2m(E - V)/\hbar^2}$ and $k = \sqrt{2mE/\hbar^2}$ and h_ℓ, j_ℓ are the Bessel-Ricatti functions.

Let $E' = E_{pole} - i\Gamma/2$ be the root of the function $H(E)$, this root is the pole of the Green function. If the pole lies either on the first or on the fourth quadrant, we have a

resonant shape of the strength function $S(E)$ in the positive energy axis. In this region, E_{pole} is positive, but the imaginary part of E can be positive or negative.

By definition we have $H(E') = 0$. If Γ is small then for every E near to E_{pole} the function $H(E)$ admits a Taylor expansion:

$$H(E) = (E - E')H'(E') + O((E - E')^2)$$

We can calculate the derivative of the function $H(E)$ at $E = E'$:

$$H'(E') = \frac{mR}{\hbar^2} \frac{V}{E' - V} \left(\tau_\ell^2(k'R) + \frac{l(l+1)}{(k'R)^2} + \frac{i\tau_\ell(k'R)}{(k'R)} \right)$$

where $k' = \sqrt{2mE'/\hbar^2}$ and the function $\tau_\ell(z)$ is defined as:

$$\tau_\ell(z) = \frac{h'_\ell(z)}{ih_\ell(z)}$$

From eqn.(6) the strength function $f_{\ell,j}^L(E)$ in the vicinity of the E can be expanded in a Laurent series as follows:

$$f_{\ell,j}^L(E) = \frac{D}{E - E'} + F + \dots \quad (8)$$

where

$$D = \frac{2}{R} \frac{E' - V}{V} \frac{\Sigma_{\ell,j}^L(E')}{\tau_\ell^2(k'R) + \ell(\ell+1)/(k'R)^2 + i\tau_\ell(k'R)/(k'R)}$$

The first term in the left hand side of (8) is proportional to $1/(E - E')$ and the second one is constant if E is in the vicinity of $E_{pole} = Re E'$. The other terms are very small and they are proportional to $(E - E')$. The first term generates the resonant peak of the response function $S(E)$, see eqn.(1), for a given configuration $[\ell, j]_\Sigma$. We can write the strength function $S(E)$ as the sum of two terms.

$$S(E) = S_p(E) + S_b(E)$$

The first term $S_p(E)$ is responsible for the peak structure, while the second term $S_b(E)$ corresponds to the continuum background. The maximum of the $S_p(E)$ is the peak which is located at E_{peak} . The $S_p(E)$ is given by the formula:

$$S_p(E) = -\frac{1}{\pi} Im\left(\frac{D}{E - E'}\right)$$

This function has two extrema,(see fig.3). In our problem, we are interested only in the maximum. We have two cases:

(i.) $Im(E') = -\Gamma/2 > 0$

Then, the location of the peak is given by the relation:

$$E_{peak} = E_{pole} + (\Gamma/2) \cot(\alpha/2) \quad (9)$$

where $\alpha = \arg(D)$.

The maximum of the resonant part $S_p(E_{peak})$ is easily estimated

$$S_p(E_{peak}) = \frac{(ImD)^2}{\pi |\Gamma| (|D| + ReD)} \quad (10)$$

(ii.) $Im(E') = -\Gamma/2 < 0$

Then, the location of the peak, E_{peak} , is:

$$E_{peak} = E_{pole} - (\Gamma/2) \tan(\alpha/2) \quad (11)$$

The corresponding value of the production strength is given by the formula:

$$S_p(E_{peak}) = \frac{(ImD)^2}{\pi |\Gamma| (|D| - ReD)} \quad (12)$$

The width ΔE of the resonant part $S_p(E)$ can be calculated and the following simple relation is valid in both cases :

$$\Delta E = 2\sqrt{2(E_{peak} - E_{pole})^2 + (\Gamma/2)^2} \quad (13)$$

If Γ is close to zero, then E_{peak} coincides with E_{pole} . This is true when the pole of the Green function is located near the real energy axis ($\Gamma = 0$). From eqn.(10) and (12) we see that in this case , the peak is very sharp and from eqn.(13) the width is very small.

In fig.4 we see that the poles of the Green function form a trajectory in the complex E-plane, when the strength of the spin-orbit potential depth V_{so} is increased. For large values of the spin-orbit interaction ,the poles approach the real energy axis.

The correlation between the positions of the poles and of the resonant peaks can be studied graphically. We define the mean potential:

$$\hat{V} = \frac{3}{R^3} \int_0^\infty V(r) r^2 dr$$

In our model

$$\hat{V} = V_c - 3V_{so}(\bar{l} \cdot \bar{s})/A^{2/3} \quad (14)$$

In fig.5 it is shown how the difference ($E_{pole} - E_{peak}$) depends on the relative ratio of the imaginary part over the mean potential:

$$\frac{|Im\hat{V}|}{|\hat{V}|} \quad (15)$$

E_{pole} is the real part of the energy eigenvalue and E_{peak} is the Sigma energy corresponding to the maximum of the associated resonance. The curve, in fig.5, corresponds to the $[d_{5/2}]_{\Sigma}$ configuration and the spin orbit well depth takes values from 0 to 40 MeV. In this case, when the spin-orbit potential increases, the real part of the mean potential is increased comparatively to the imaginary part and the ratio in eqn.(15) decreases. We notice that the position of the real part of the energy eigenvalue approaches the position of the peak, when the real part is greater than the corresponding imaginary part of the potential.

Equation (14) indicates that the spin-orbit effects should be stronger in the hypernuclei with relatively low mass number A. The appearance of a strong peak is more probable for small A, see ref.[11].

To each Sigma configuration corresponds a partial resonant peak and the superposition of these partial peaks creates the total spectrum. The position of each partial resonant peak corresponds to the real part of the energy eigenvalue, though it does not necessarily coincide with it. Therefore the resonance due to $[d_{5/2}]_{\Sigma}$ is closer to the energy threshold than the $[d_{3/2}]_{\Sigma}$ resonance or the $[f_{7/2}]_{\Sigma}$ resonance (see fig.2).

For a given ℓ , the contribution from the $j = \ell + \frac{1}{2}$ hyperon configuration gives a peak closer to the energy threshold, than the corresponding $j = \ell - \frac{1}{2}$ hyperon configuration, whose peak is located far away from the Sigma threshold. If the spin orbit potential is real and positive, from eqn.(14) we conclude that the absolute value of the mean real potential, for the $j = \ell + \frac{1}{2}$ configuration, is greater than the mean real potential of the $j = \ell - \frac{1}{2}$ configuration. Therefore the peaks of the $j = \ell + \frac{1}{2}$ configurations are sharper and lie nearer the threshold than the corresponding peaks of the $j = \ell - \frac{1}{2}$ configurations, for the same l (see fig.2).

Calculations of the at rest spectrum have been given with the Woods-Saxon optical potential by Morimatsu and Yazaki [18] and the essential features of the $(K, \pi^{\pm})_{\Sigma}$ -hypernuclear spectrum are the same, with those obtained in our case.

In fig.6, we draw the at-rest π -spectrum for different values of the spin-orbit potential. We remark that the peaks of the different Σ configurations appear more clearly when the value of the spin-orbit parameter is augmented. In this case the quantity (15) is decreased. The corresponding resonant peaks for each Σ configuration become sharper.

An eventual experimental confirmation of the existence of the peaks in the spectrum must be connected to relatively low values of the imaginary part of the potential and/or to

a strong real spin-orbit potential. The absence of the peaks in the experimental spectrum indicates the importance of the Σ to Λ conversion and a relatively moderate real and/or a complex spin-orbit potential.

3. Conclusions

The study of the Green function part of the production strength leads to the following conclusions:

- i. The existence of narrow resonant peaks can be related to large real values of the spin-orbit potential and to a relatively low Σ to Λ conversion.
- ii. The theory of the poles of the hypernuclear Green function can be used to explain qualitatively the gross features of the spectrum as the superposition of partial resonances, which correspond to definite hyperon configurations.
- iii. The resonant behaviour in the spectrum originates mainly from the Green function part of the the strength function . This part is independent of the original creation mechanism of the sigma hypernuclei.

Calculations of the $(K, \pi^\pm)_\Sigma$ -hypernuclear spectrum with other models, lead also to the conclusion that, when a large real potential with large spin-orbit interaction is used, we have bound Sigma-hypernuclear states [20-23], with a small quasifree process [22,23].

REFERENCES

- [1]. R.Bertini et al. Phys.Lett. **90B** (1980) 375
- [2]. H.Piekarz et al. Phys.Lett. **110B** (1982) 428
- [3]. R.Bertini et al. Phys.Lett. **136B** (1984) 29
- [4]. R.Bertini et al. Phys.Lett. **158B** (1985) 19
- [5]. E.V.Hungerford Nucl.Phys. **A450** (1986) 157
- [6]. T.Yamazaki et al. Phys.Rev.Lett. **54** (1985) 102
- [7]. T.Yamazaki et al. Nucl.Phys. **A450** (1986) 1c
- [8]. R.S.Hayano et al. *Proceedings of the INS symposium on Hyper nuclear physics* , Tokyo 1986, p.19
- [9]. S.Paul et al. Nucl.Phys. **A479** (1988) 137c
- [10]. H.Tamura et al. Nucl.Phys. **A479** (1988) 161c
- [11]. R.S.Hayano et al. Phys.Lett. **231B** (1989) 355c
- [12]. A.Gal, G.Toker and Y.Alexander Ann.of Phys.(NY) **137** (1981) 341
- [13]. C.J.Batty, A.Gal and G.Toker Nucl.Phys. **A402** (1983) 349
- [14]. O.Morimatsu and K.Yazaki Nucl.Phys. **A435** (1985) 727
- [15]. A.Gal Nucl.Phys. **A450** (1986) 343c
- [16]. T.Kishimoto Nucl.Phys. **A450** (1986) 447c

- [17]. R.E.Chrien, E.V.Hungerford and T.Kishimoto, Phys.Rev. **35C** (1987) 1589
- [18]. O.Morimatsu and K.Yazaki, Nucl.Phys. **A483** (1988) 493
- [19]. E.H.Auerbach et al., Ann.Phys. **148** (1983) 381
- [20]. R.Hausmann and W.Weise,Z.Physik **A324** (1986) 355
- [21]. M.Kohno et al. Nucl.Phys. **A470** (1987) 609
- [22]. J.Zofka *Proceedings of the INS symposium on Hyper nuclear physics*, Tokyo 1986, p.97
- [23]. R.Wunsch and J.Zofka *Proceedings of the INS symposium on Hypernuclear physics*, Tokyo 1986, p.17

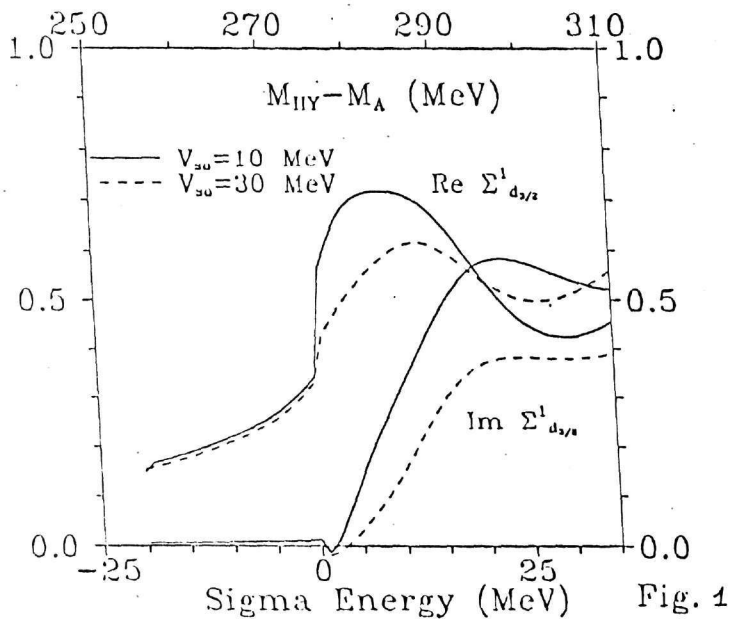


Fig. 1. The $\Sigma_{d_{3/2}}^1(E)$ of eqn.(7), for $V_{su} = 0$ and 30 MeV .

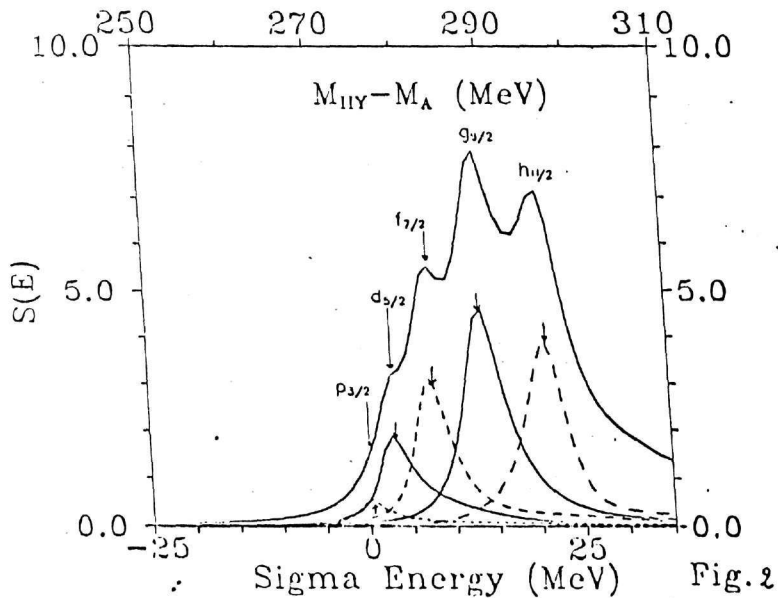


Fig. 2. The production strength $S(E)$, when $V_c = -12 - i6 \text{ MeV}$ and $V_{su} = 35 \text{ MeV}$.

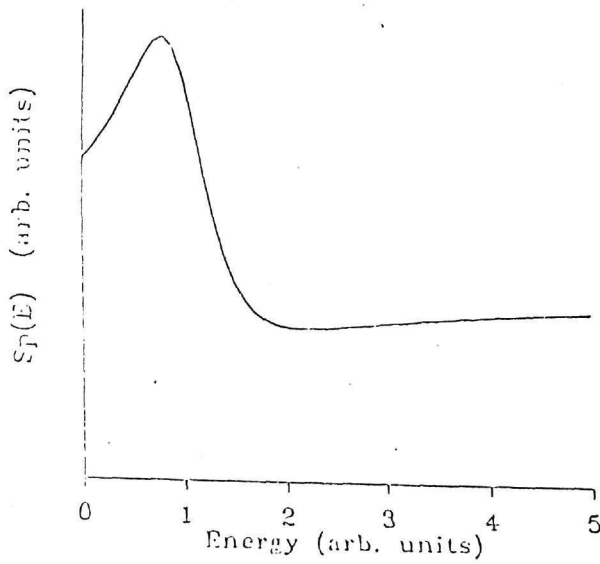


Fig. 3

Fig. 3. The resonant part of the production strength $S_T(E)$, as function of E .

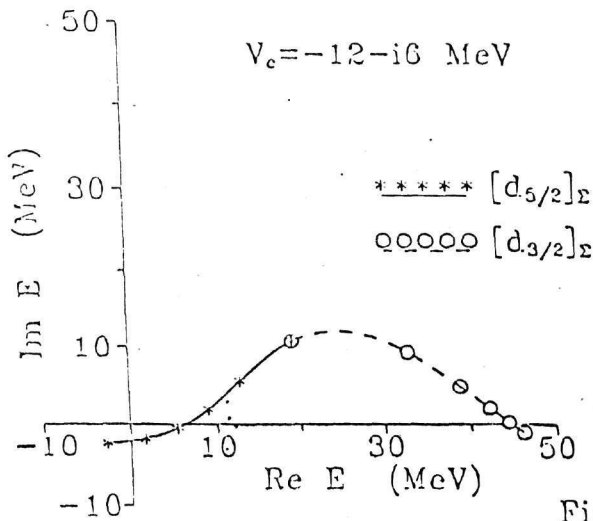


Fig. 4

Fig. 4. The position of the poles in the E -plane, when the central potential parameter is $V_c = -12 - i6 \text{ MeV}$ and the spin-orbit parameter varies, $V_{so} = 0, 10, \dots, 50 \text{ MeV}$. The common point of the $[d_{5/2}]_\Sigma$ (solid) curve and of the $[d_{3/2}]_\Sigma$ (dashed) curve corresponds to $V_{so} = 0 \text{ MeV}$.

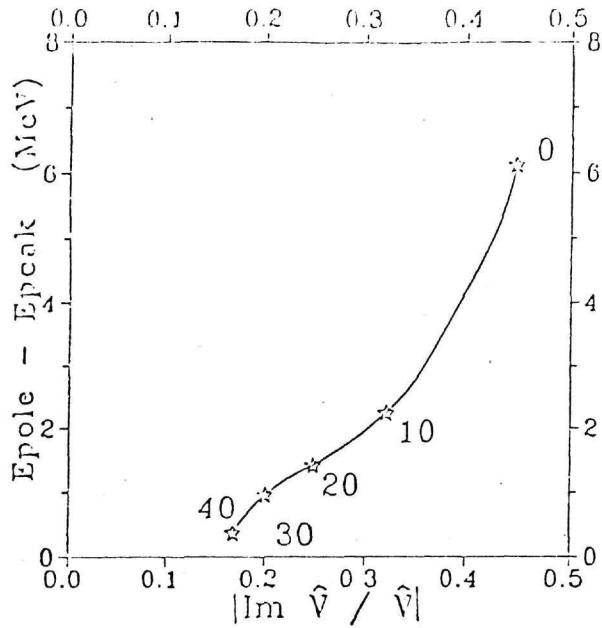


Fig. 5

Fig. 5. The central potential parameter is $V_c = -12 - i6$ MeV and the spin-orbit parameter varies, $V_{so} = 0, 10, \dots, 50$ MeV. When V_{so} increases the $(E_{\text{peak}} - E_{\text{pole}})$ decreases.

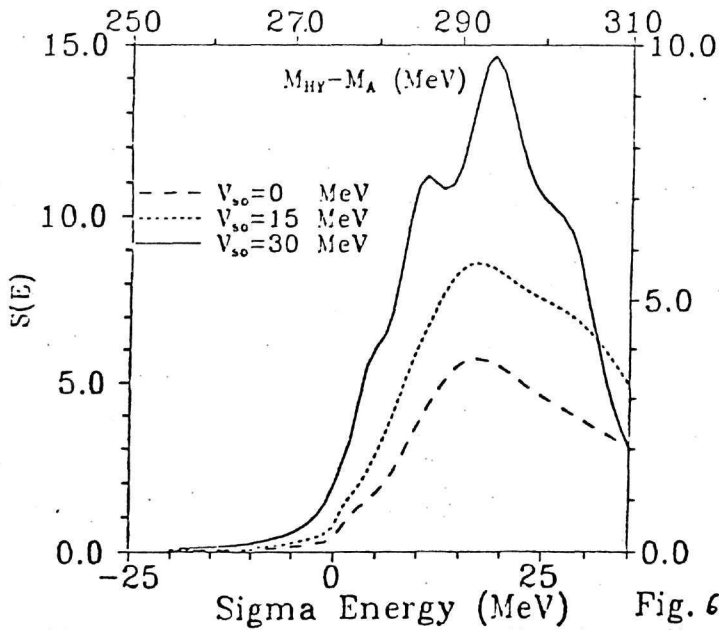


Fig. 6.

Fig. 6. The production strength $S(E)$ for $V_c = -12 - i6$ MeV and the spin-orbit parameter varies, $V_{so} = 0, 10, 30$ MeV.